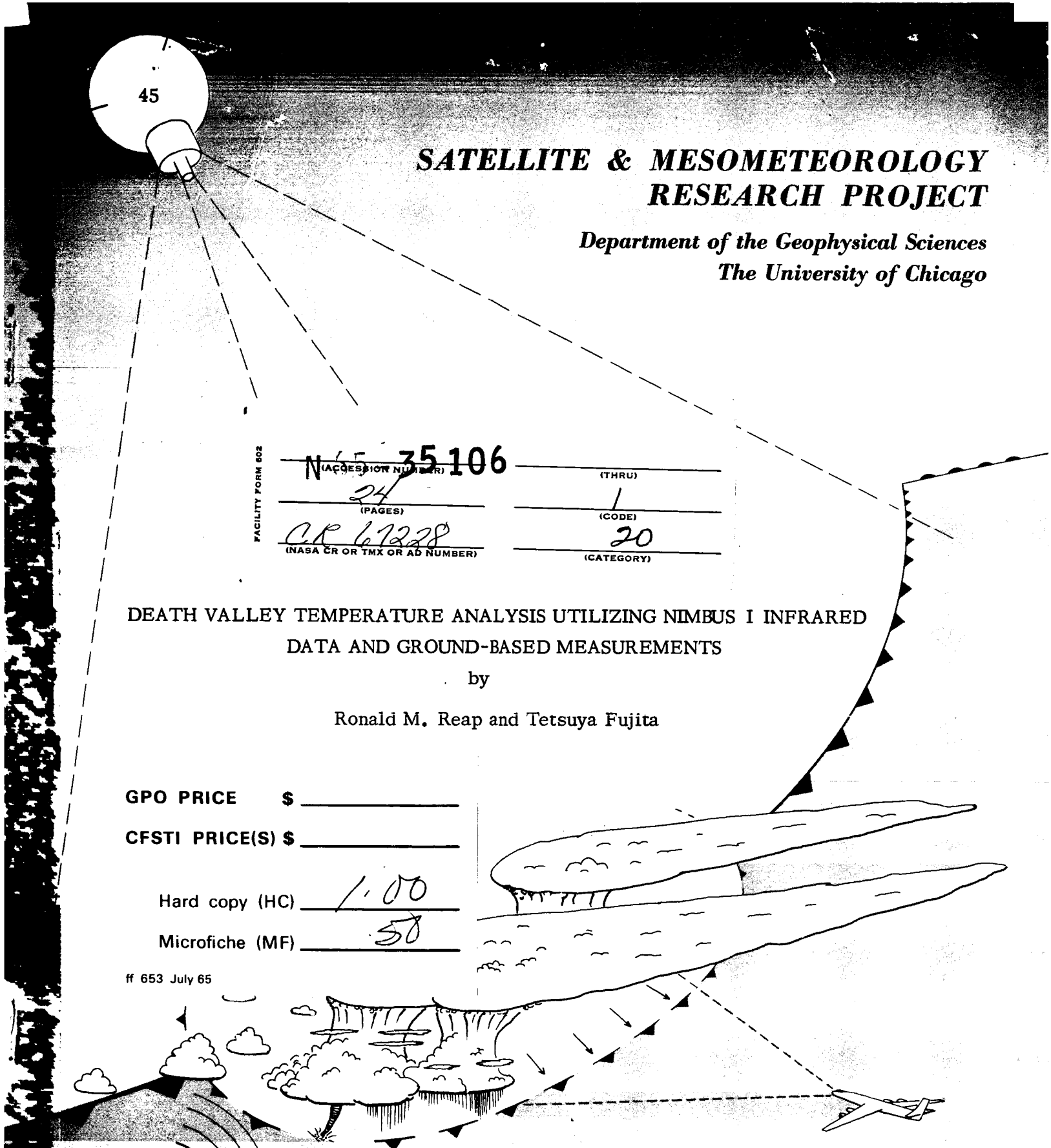

SATELLITE & MESOMETEOROLOGY RESEARCH PROJECT

Department of the Geophysical Sciences
The University of Chicago

DEATH VALLEY TEMPERATURE ANALYSIS UTILIZING NIMBUS I INFRARED DATA AND GROUND-BASED MEASUREMENTS

by

Ronald M. Reap and Tetsuya Fujita

SMRP Research Paper

NUMBER 45

August 1965

MESOMETEOROLOGY PROJECT ---- RESEARCH PAPERS

1.* Report on the Chicago Tornado of March 4, 1961 - Rodger A. Brown and Tetsuya Fujita

2.* Index to the NSSP Surface Network - Tetsuya Fujita

3.* Outline of a Technique for Precise Rectification of Satellite Cloud Photographs - Tetsuya Fujita

4.* Horizontal Structure of Mountain Winds - Henry A. Brown

5.* An Investigation of Developmental Processes of the Wake Depression Through Excess Pressure Analysis of Nocturnal Showers - Joseph L. Goldman

6.* Precipitation in the 1960 Flagstaff Mesometeorological Network - Kenneth A. Styber

7.** On a Method of Single- and Dual-Image Photogrammetry of Panoramic Aerial Photographs - Tetsuya Fujita

8. A Review of Researches on Analytical Mesometeorology - Tetsuya Fujita

9. Meteorological Interpretations of Convective Nephsystems Appearing in TIROS Cloud Photographs - Tetsuya Fujita, Toshimitsu Ushijima, William A. Hass, and George T. Dellert, Jr.

10. Study of the Development of Prefrontal Squall-Systems Using NSSP Network Data - Joseph L. Goldman

11. Analysis of Selected Aircraft Data from NSSP Operation, 1962 - Tetsuya Fujita

12. Study of a Long Condensation Trail Photographed by TIROS I - Toshimitsu Ushijima

13. A Technique for Precise Analysis of Satellite Data; Volume I - Photogrammetry (Published as MSL Report No. 14) - Tetsuya Fujita

14. Investigation of a Summer Jet Stream Using TIROS and Aerological Data - Kozo Ninomiya

15. Outline of a Theory and Examples for Precise Analysis of Satellite Radiation Data - Tetsuya Fujita

* Out of print
** To be published

(Continued on back cover)

SATELLITE AND MESOMETEOROLOGY RESEARCH PROJECT
Department of the Geophysical Sciences
The University of Chicago

DEATH VALLEY TEMPERATURE ANALYSIS UTILIZING NIMBUS I INFRARED DATA AND GROUND-BASED MEASUREMENTS

by

Ronald M. Reap and Tetsuya Fujita

SMRP Research Paper #45

August 1965

The research reported in this paper has been supported by the National Aeronautics and Space Administration under grant NASA NsG 333.

DEATH VALLEY TEMPERATURE ANALYSIS UTILIZING NIMBUS I INFRARED DATA AND GROUND-BASED MEASUREMENTS

Ronald M. Reap and Tetsuya Fujita

Department of the Geophysical Sciences

The University of Chicago

Chicago, Illinois

35106

ABSTRACT

During February, 1965 a series of temperature and radiation measurements were made within Death Valley by Colorado State University. Members of the Satellite and Mesometeorology Research Project of the University of Chicago assisted in the field operations by precisely locating and photographing thermograph and surface temperature sites which had been established in the area. Since the measured temperatures depend upon instrument location, a detailed description is given of the terrain features surrounding the sites. A temperature analysis of Death Valley and the Sierra Nevada range was also made utilizing Nimbus I HRIR data and mean shelter temperatures recorded at five synoptic stations in the area.

author

1. Introduction

On August 28, 1964 the first meteorological satellite in the Nimbus series was launched into a quasi-polar orbit. The orbital characteristics of Nimbus I provided near local noon cloud photography by the Advanced Vidicon Camera Subsystem (AVCS) and near local midnight radiation measurements by the High Resolution Infrared Radiometer (HRIR). The HRIR carried by Nimbus I was spectrally sensitive in the 3.4 to 4.2 micron near-infrared window and was designed to produce detailed cloud-cover pictures of the dark side of the earth.

Assuming a surface emissivity of 1.0, a zenith angle of 0°, and cloud-free conditions, Kunde (1964) has theoretically calculated the magnitude of atmospheric absorption in the 3.4 to 4.2 micron near-infrared band for several model atmospheres. The attenuation of outgoing infrared radiation in this band results from weak absorption by atmospheric CO_2 and H_2O. A difference of 0.5C to 2.0C was found to exist between

---

The research reported in this paper has been supported by the National Aeronautics and Space Administration under grant NASA NsG 333.

the assumed mid-latitude surface temperatures and equivalent blackbody temperatures corresponding to the calculated infrared energy escaping into space. The spectral range of the Nimbus I HRIR thus corresponds to a very clean atmospheric window and the observed radiation intensities should provide an excellent indication of the actual surface temperatures and mesoscale temperature gradients.

As demonstrated by Fujita and Bandeen (1965), the HRIR subsystem has significantly increased the quality of radiational mapping obtainable from the original satellite analog traces. This increase in mapping detail resulted from the clean atmospheric window and the 0.45^{o} field-of-view resolution offered by the Nimbus I radiometer as compared to 5.0^{o} for the preceding TIROS satellites.

2. Comparison of Nimbus I Radiation Analysis and Shelter Temperatures

Observation by Nimbus I of the dry and cloud-free southwest United States during overpass of Orbit 73 on 2 September has provided some interesting radiational profiles resulting from pronounced topographic features such as Grand Canyon, Death Valley and the Sierra Nevada range. By analyzing a section of the foregoing region, Fujita and Bandeen (1965) have shown that a high degree of correlation exists between terrain height and the actual Nimbus I surface temperature measurements. Their equivalent blackbody surface temperatures were obtained by applying a 1^{o} (scan angle) running mean smoothing technique to the original satellite analog traces.

Death Valley was especially noteworthy because of the high temperatures and mesoscale temperature gradients observed by Nimbus I. Figure 1 shows the mean equivalent blackbody temperature analysis as obtained from the calibrated Nimbus I analog traces while Fig. 2 gives the corresponding topographic map. Inspection reveals an excellent correlation between terrain height and temperature. The surface temperatures ranged from -12C for Mt. Whitney (14,495 ft msl) to 18C for Death Valley, which are, respectively, the highest and lowest land areas in the contiguous 48 states. The maximum observed surface temperature corresponded to that section of Death Valley ranging in elevation from -200 to -282 ft msl. Dry lakes and small bodies of water located at relatively low elevations, such as Owens Lake and the Haiwee Reservoirs in Owens Valley, stand out as warm areas in the near midnight (1145 PST) radiation analysis. The strongest surface temperature gradients were found to coincide with the slope of the Sierra Nevada range from the floor of Owens Valley to Mt. Whitney and the slope from Death Valley to Telescope

Peak in the Panamint Range. Figure 3 shows an enlarged HRIR picture of Death Valley and the Sierra Nevada range corresponding to the radiation analysis given in Fig. 1.

Figure 4 illustrates the shelter temperature versus station height profile obtained for Death Valley and several stations in the area for the years 1960 and 1962. The average values for the two-year sample reveal that the decrease in shelter temperature with an increase in station elevation corresponds closely to the value for the dry-adiabatic lapse rate. Furthermore, the Death Valley region is dominated by a hot desert climate which precludes extensive convective activity with subsequent cloudiness and precipitation. The average number of clear days per year is 283 with a mean annual precipitation of approximately 2 inches, most of which falls in winter and during a few violent summer showers. Therefore, the small seasonal and diurnal variation of cloudiness and atmospheric turbidity have a negligible effect upon the average temperatures given in Fig. 4.

As shown by the curves in Fig. 4, the mean maximum and minimum shelter temperatures for the two-year period exhibit a noticeable departure from the dry-adiabatic value. This departure reflects an increase in the daily temperature range with height resulting from relatively weak absorption of solar and terrestrial radiation by the colder and less dense atmosphere at the higher station elevations.

At the near midnight Nimbus I observation one might at first expect Death Valley to be filled with cold air. However, the infrared radiation analysis (Fig. 1) indicates a warm valley floor. Since Death Valley is in reality a large depression in the earth's surface, with an average width of 10-15 miles, the usual concept of a valley bottom filled at night with cold air does not necessarily apply. It is the authors' view that most of the effective cold air drainage at night originates from the lowest 1000 ft of mountain slope. However, as shown by Fig. 7, this lower slope area is small in comparison to the large areal extent of Death Valley. The lack of well-developed cold drainage winds is especially evident during the hot summer months when the minimum shelter temperatures are often only a few degrees lower than the maximum daytime temperatures.

In Fig. 5, satellite-measured surface temperatures are plotted against the corresponding terrain heights. A unique relationship between the surface temperatures and topography is again clearly demonstrated. The point values in the scatter plot were obtained by carefully selecting areas of relatively flat ground at various elevations and locating the proper temperatures from the radiation analysis. Rugged topography, such as steep mountain ridges interspersed with narrow valleys, was generally avoided

in preparing the scatter diagram. In such cases, the radiative intensities measured by the satellite correspond to an effective terrain height which is rather difficult to estimate.

The instantaneous lapse rate of surface temperature given in Fig. 5 is approximately 8.5C/km, as compared to the dry-adiabatic lapse rate of 10C/km. The temperature profile measured by Nimbus I at 1145 PST (Fig. 5) thus represents a transition stage between the mean maximum and minimum shelter temperatures as given, respectively, by the dashed and dash-dotted curves in Fig. 4. This implicitly assumes uniform soil emissivities and a fairly constant difference between the shelter and surface temperatures with increasing elevation.

3. Description of Death Valley Temperature and Radiation Measurements

In order to investigate the temperature and radiation profiles within Death Valley, a series of measurements were made during February 1965 by Marlatt* of Colorado State University. A map of Death Valley and adjacent deserts and mountain ranges is shown in Fig. 7. The locations numbered from 1-7 correspond to thermograph sites (Fig. 6) located at approximately 1000-ft intervals from a 6000-ft msl elevation near Aguerreberry Point to the valley floor. Figure 8 gives a panoramic view from Aguerreberry Point looking eastward across Death Valley while Figs. 9-15 show the various thermograph sites positioned down Trail Canyon to the Devils Golf Course. The sites were established to provide data on the 24-hour temperature profiles at varying elevations above the valley floor. Infrared radiation emitted by the canyon floor and surrounding walls near the thermograph sites was also recorded during the 24-hour study by a hand-carried 8-13 micron radiometer.

At points A and B in Fig. 7, a network of 20 electronic thermistors was established over a circle of 100-ft radius to measure surface temperatures. Figure 9 illustrates the surface temperature site at the Devils Golf Course. In addition, a medium resolution radiometer with an 8-13 micron filter was flown over points A and B by a Piper Twin Comanche aircraft. The surface temperature measurements were taken coinciding with flyover by the aircraft at approximately three hour intervals during a 24-hour period.

The data acquired from the above experiments are now under reduction and evaluation by the Department of Atmospheric Sciences at Colorado State University.

---

*Personal communication, report to be published in near future.

4. Radiative Surface of Death Valley

Death Valley represents a vast repository containing a wide array of soil types and rock formations. Possible variations in the infrared emissivity of the widely differing surface materials led to a series of emissivity measurements by Colorado State University in conjunction with the temperature measurements described previously. A number of rock and soil samples were also obtained for laboratory examination at a later date.

Several terrain features typical of the Death Valley area are shown in Figs. 16-20. Figure 16 illustrates the sand dunes located immediately north of Stovepipe Wells. Over a period of time, dust and sand-laden winds sweeping from the north collided with the mountainous obstruction located at the bend of the valley near Stovepipe Wells. The ensuing turbulence and loss of velocity resulted in the formation of sand dunes by the fallout of windborne erosion particles over a localized area.

Figures 18-19 portray terrain at the surface temperature sites located by points A and B in Fig. 7. The Devils Golf Course (Fig. 18) represents the rugged surface of a 1000-ft thick interbedded layer of salt and water bearing gravels. Capillary action brings salt-laden water from below. Upon evaporation, a small amount of salt is deposited. Pillars of salt are eventually formed which at times may reach 18 inches to 2 ft in height. The Amargosa Desert (Fig. 19) lies at an average elevation of 2500 ft msl to the east of Death Valley. Bare Mountain forms the background in Fig. 19 while hardy desert plants, such as the creosote bush, are found in the foreground. The sandy soil is covered by a thin layer of gravel coated with "desert varnish," a darkening of the rock surface due to long exposure.

Figure 17 illustrates the salt flats immediately north of the Devils Golf Course. During the cool and moist Ice Age, a lake 100 miles long and up to 600 ft deep covered the floor of Death Valley. After the uplifting of the Sierra Nevada range to the west, ancient Lake Manly slowly evaporated leaving behind deposits of silt, clay and salt. The fresh water oasis at Furnace Creek (Fig. 20) provides a vivid contrast to the adjacent dry and relatively barren valley floor.

5. Conclusions

As indicated by a mesoscale temperature analysis of Death Valley and the

Sierra Nevada range, the Nimbus I HRIR system has provided a significant increase in the quality of radiational mapping obtainable from satellite data. A unique relationship was found to exist between the satellite-measured surface temperatures and terrain height. The instantaneous lapse rate of surface temperature was computed as 8.5C/km for the area covered by the radiation analysis. On the average, the lapse rate of shelter temperatures for five stations located at differing elevations in the area was found to closely correspond to the dry-adiabatic value.

REFERENCES

Fujita, T. and W. Bandeen, 1965: Resolution of the Nimbus High Resolution Infrared Radiometer. SMRP Research Paper 40, Univ. of Chicago, 11 pp.

Kunde, V., 1964: Theoretical relationship between the HRIR equivalent blackbody temperatures and surface temperatures. Paper presented at the 4th Western National Meeting of the American Geophysical Union held during December 28-30 at the University of Washington, Seattle, Wash.

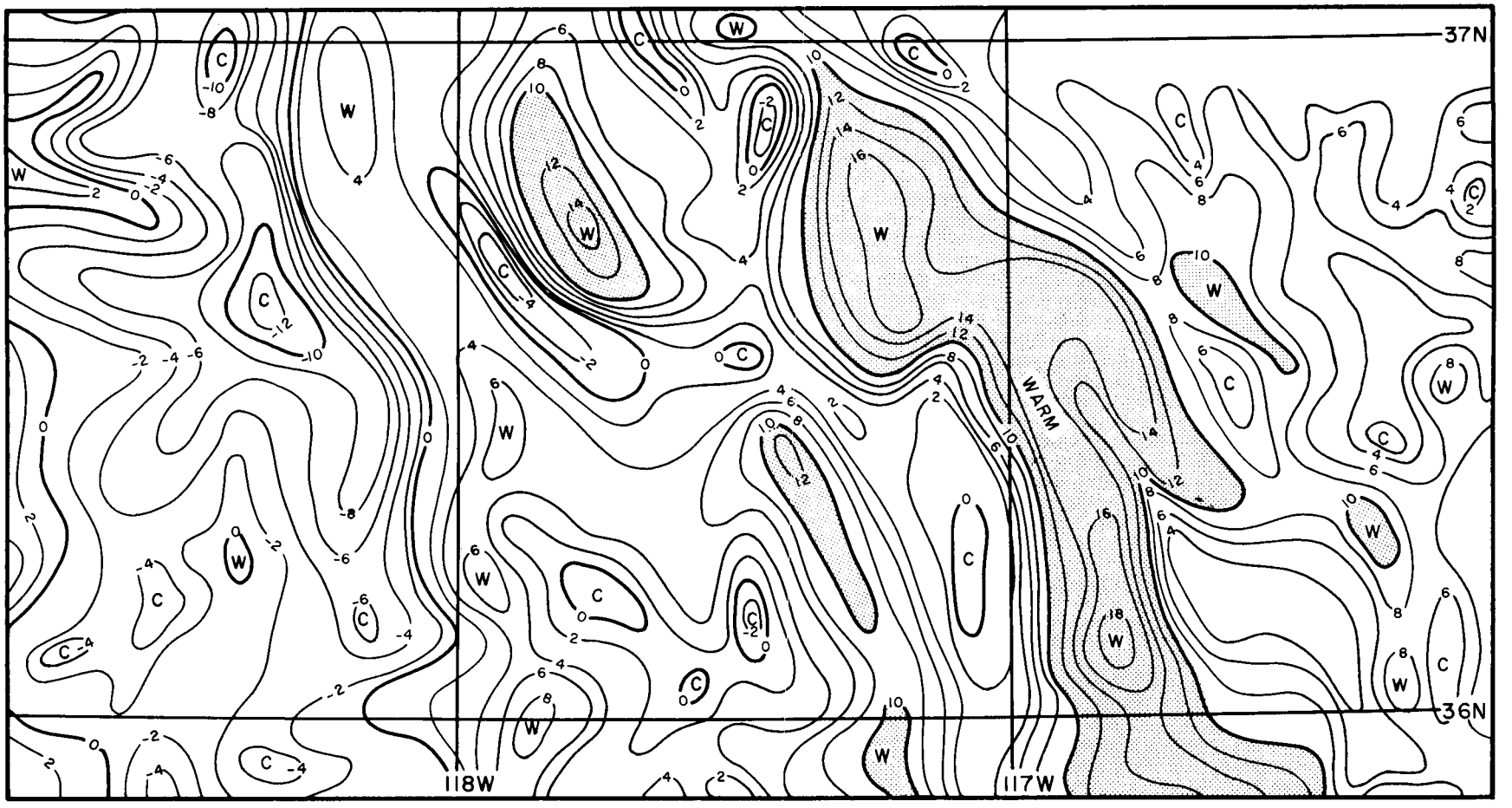

Fig. 1. Mean equivalent blackbody surface temperatures for Death Valley and the Sierra Nevada range obtained by Nimbus I during Orbit 73, September 2, 1964. Isotherms are contoured for every 2C.

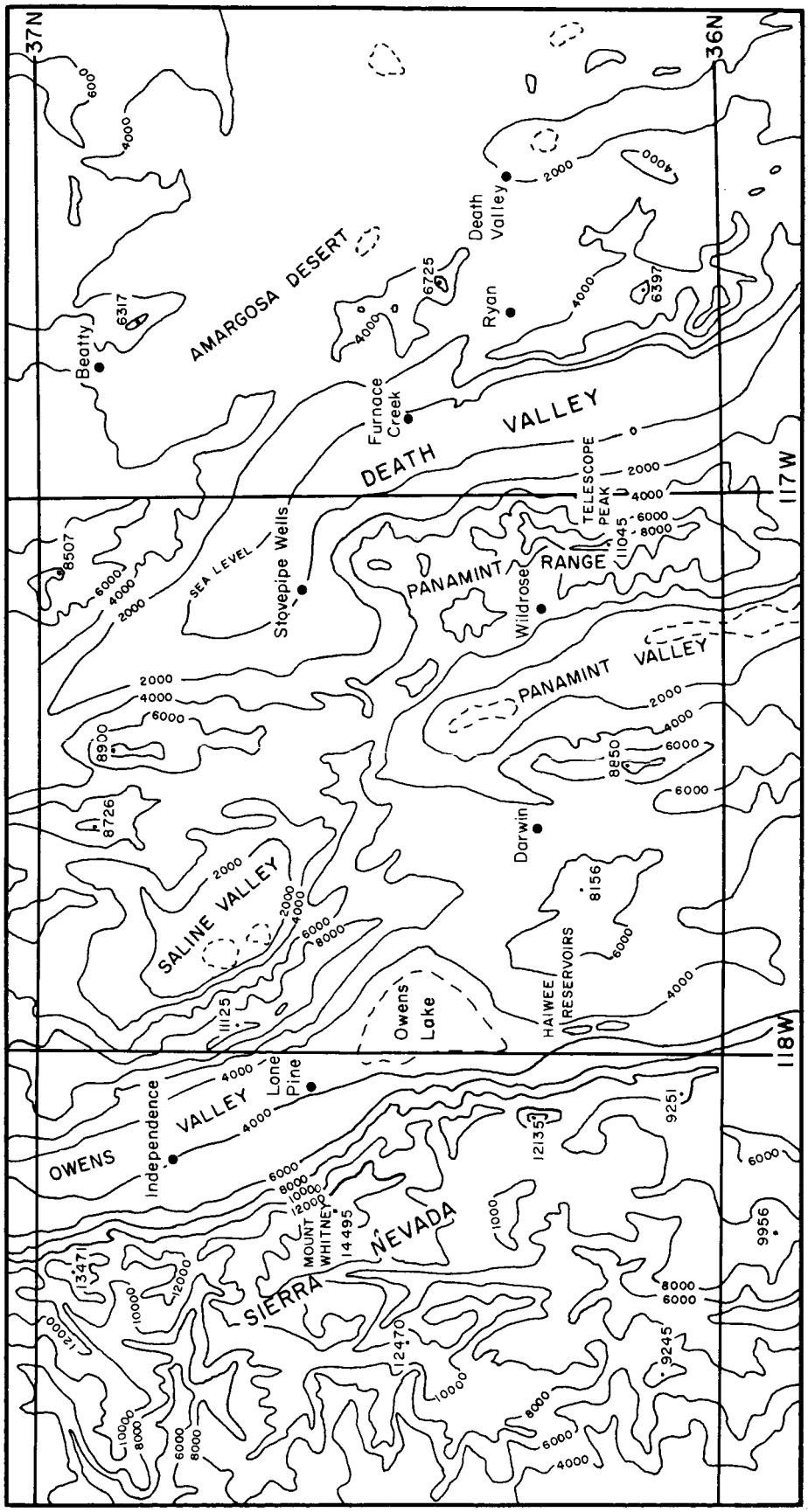

Fig. 2. Topographic map of Death Valley and the Sierra Nevada range.

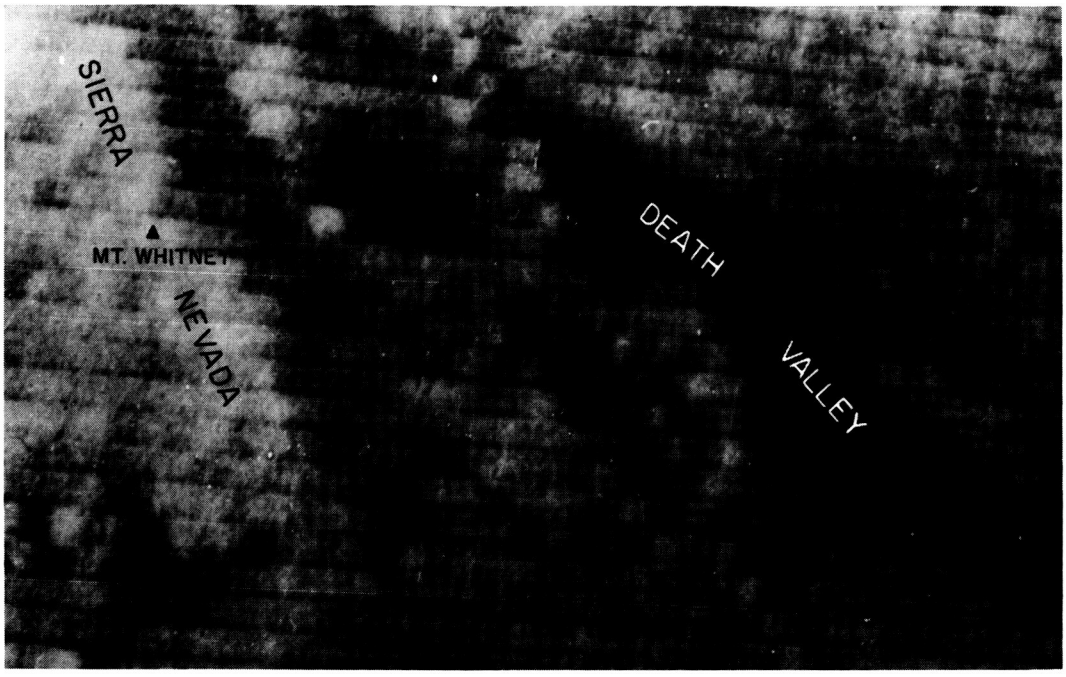

Fig. 3. Enlarged HRIR picture of Death Valley and the Sierra Nevada range corresponding to the temperature analysis given in Fig. 1.

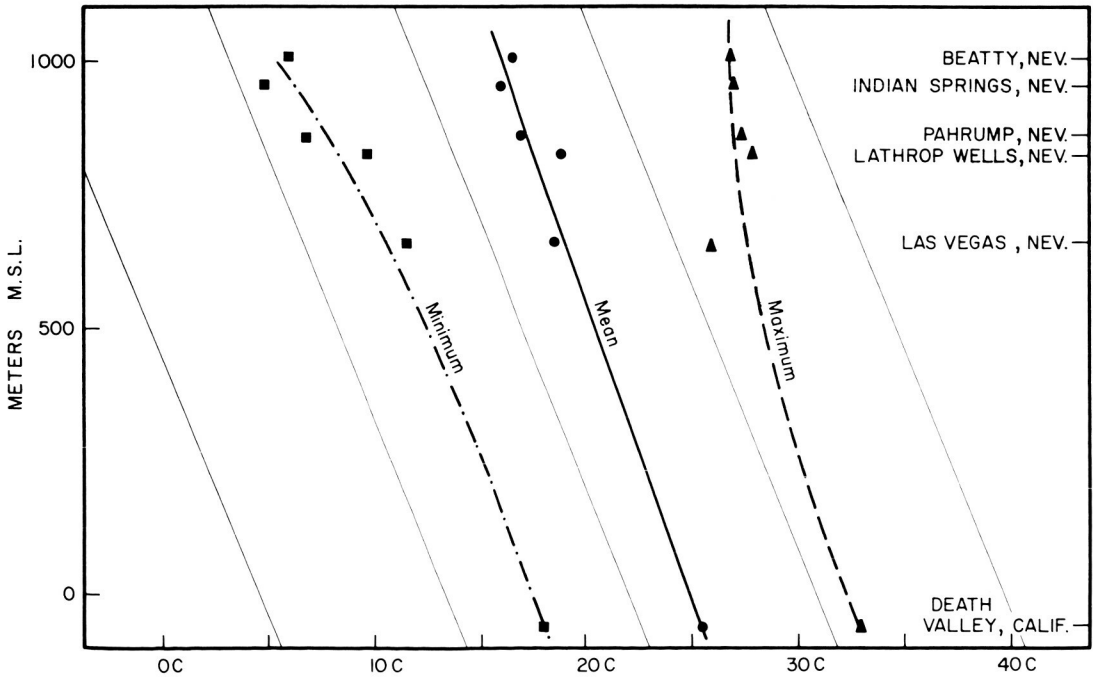

Fig. 4. Station height above msl versus the mean maximum and minimum shelter temperatures for the years 1960 and 1962. Thin sloping lines are dry-adiabats.

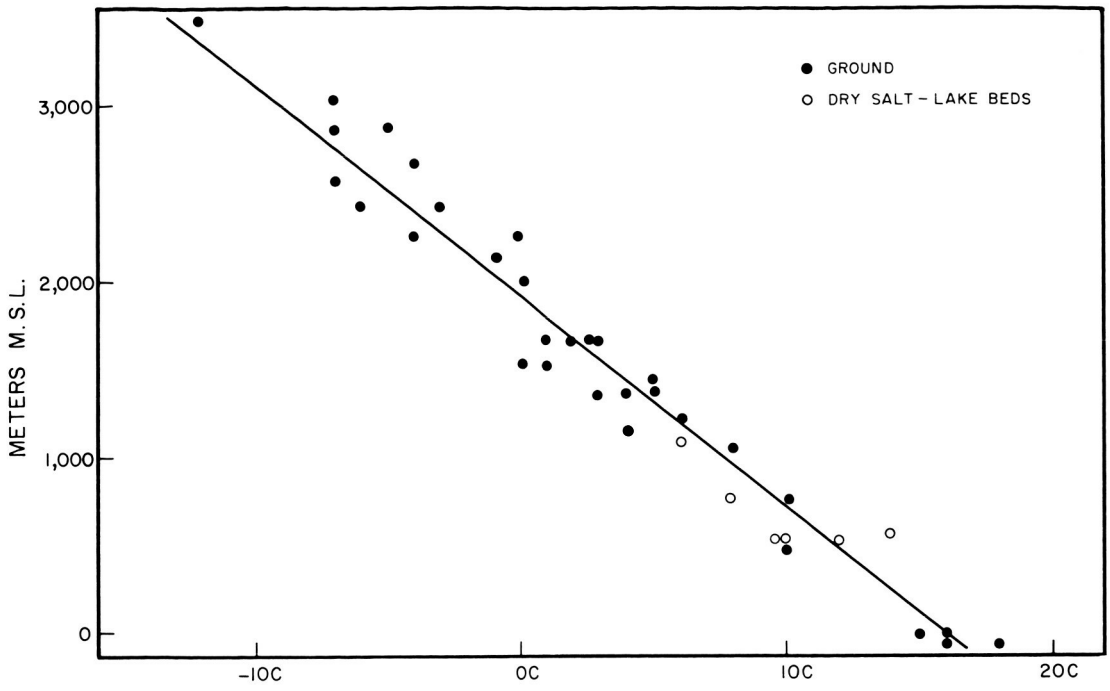

Fig. 5. Scatter diagram of terrain height and the corresponding mean equivalent blackbody surface temperatures measured by Nimbus I.

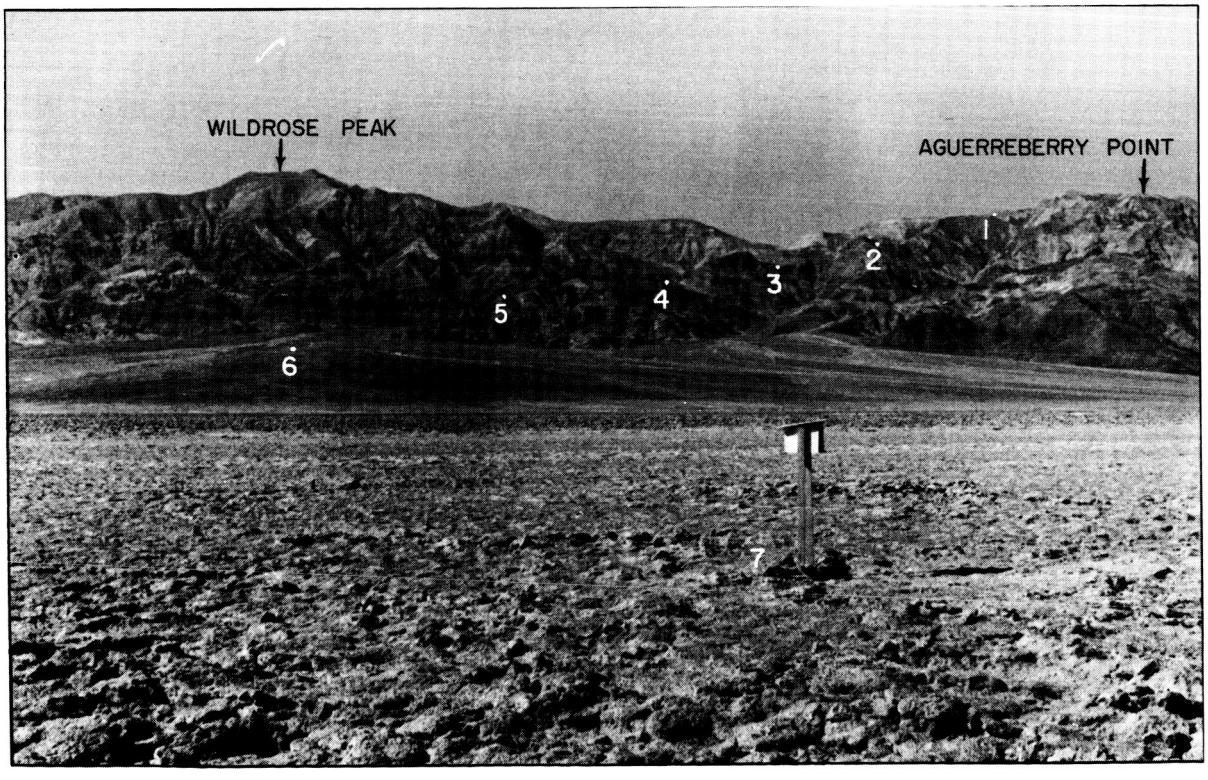

Fig. 6. Numbers 1-7 correspond to thermograph sites located at 1000-ft intervals from a 6000-ft msl elevation near Aguerreberry Point to the floor of Death Valley.

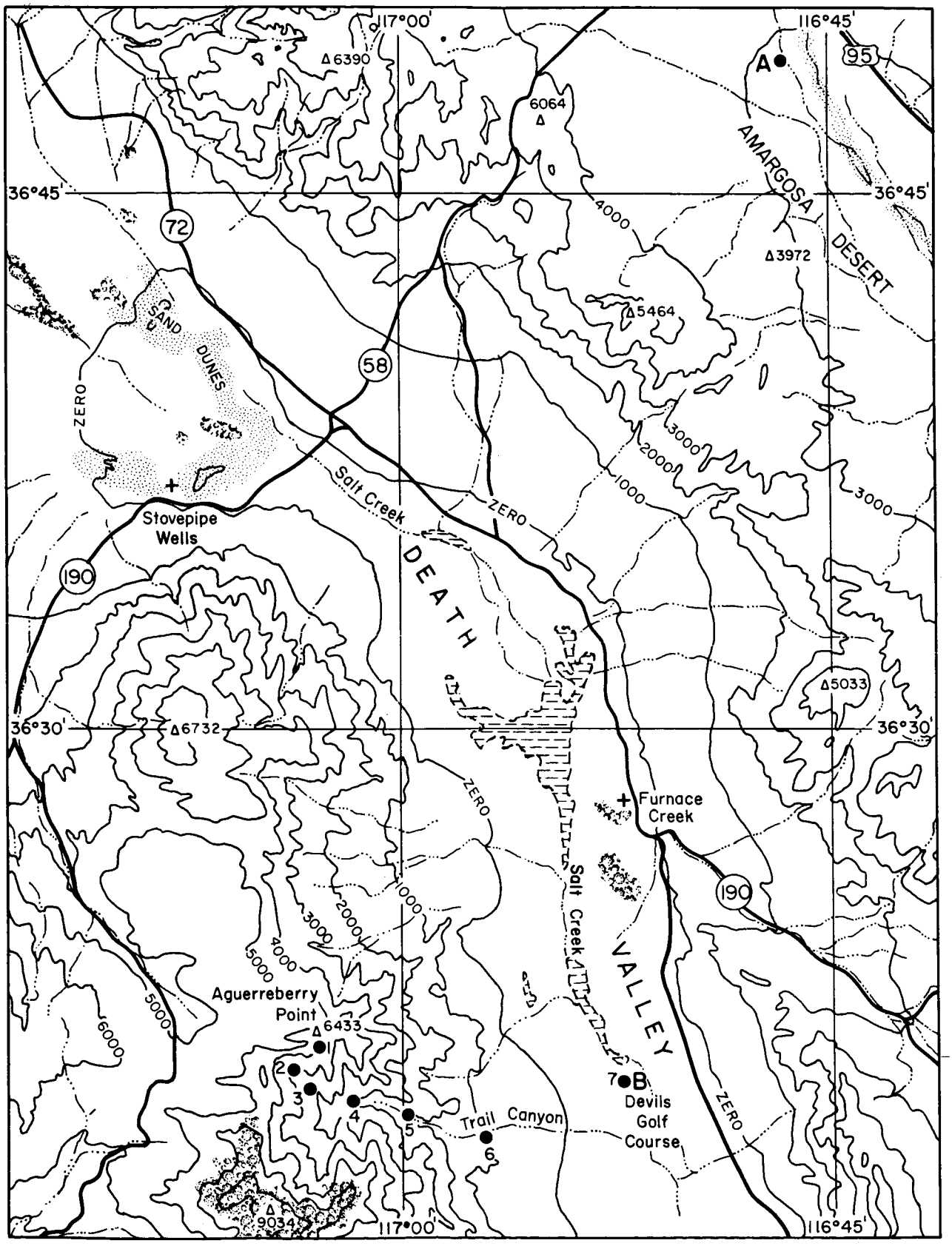

Fig. 7. Detailed map of Death Valley and adjacent mountain ranges.

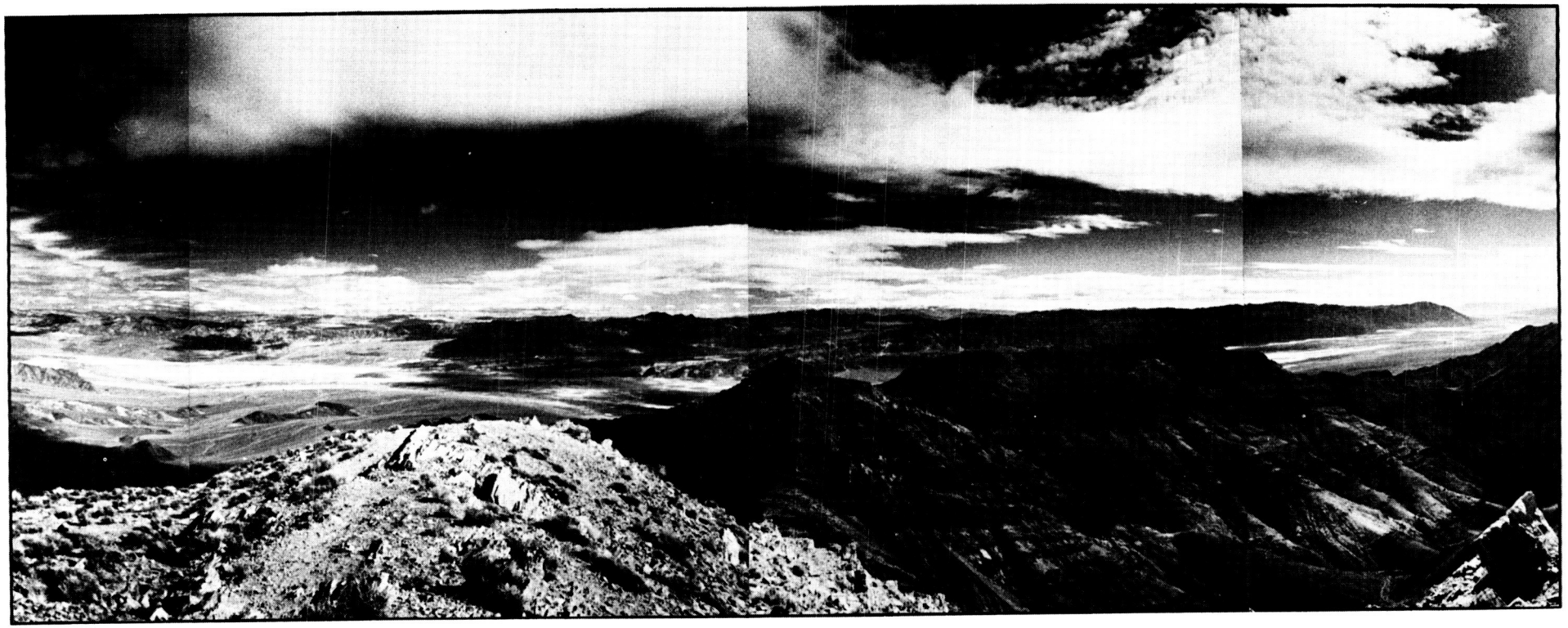

Fig. 8. Panoramic view from Aguerreberry Point looking eastward across Death Valley.

Fig. 9. Thermograph site No. 7 and surface temperature equipment located on the Devils Golf Course at an elevation of -260 ft msl.

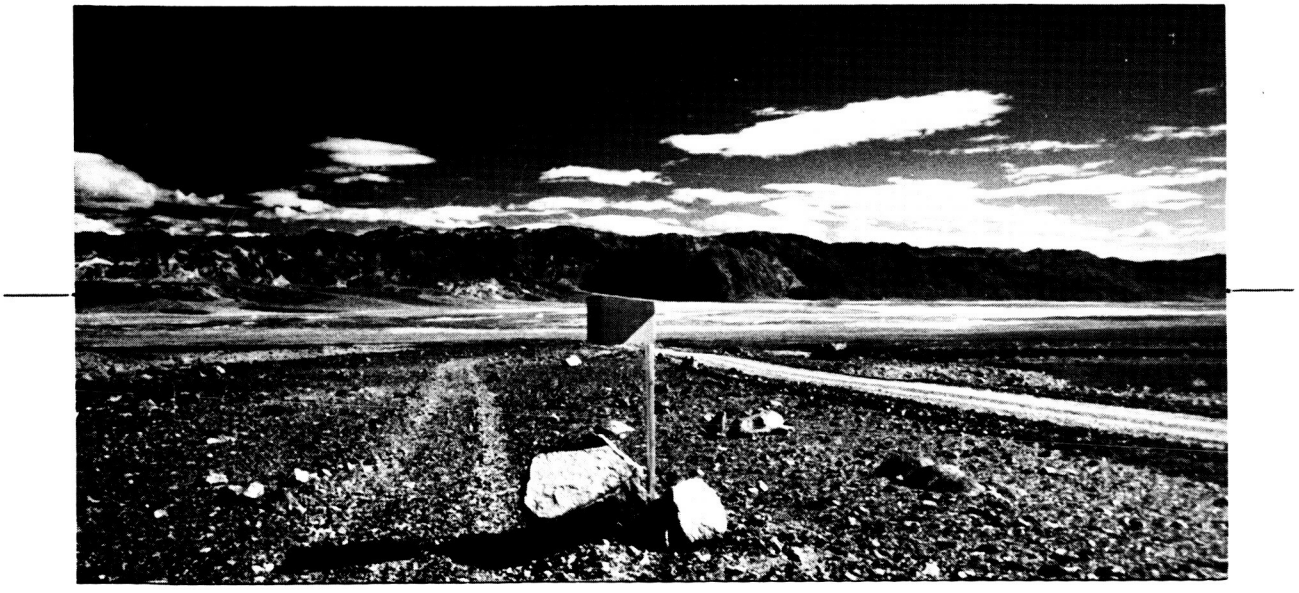

Fig. 10. Thermograph site No. 6 located at an elevation of 1000 ft msl. Horizon is indicated by ticks on the photograph border.

Fig. 11. Thermograph site No. 5 located at an elevation of 2000 ft msl.

Fig. 12. Thermograph site No. 4 located at an elevation of 3000 ft msl.

Fig. 13. Thermograph site No. 3 located at an elevation of 4000 ft msl.

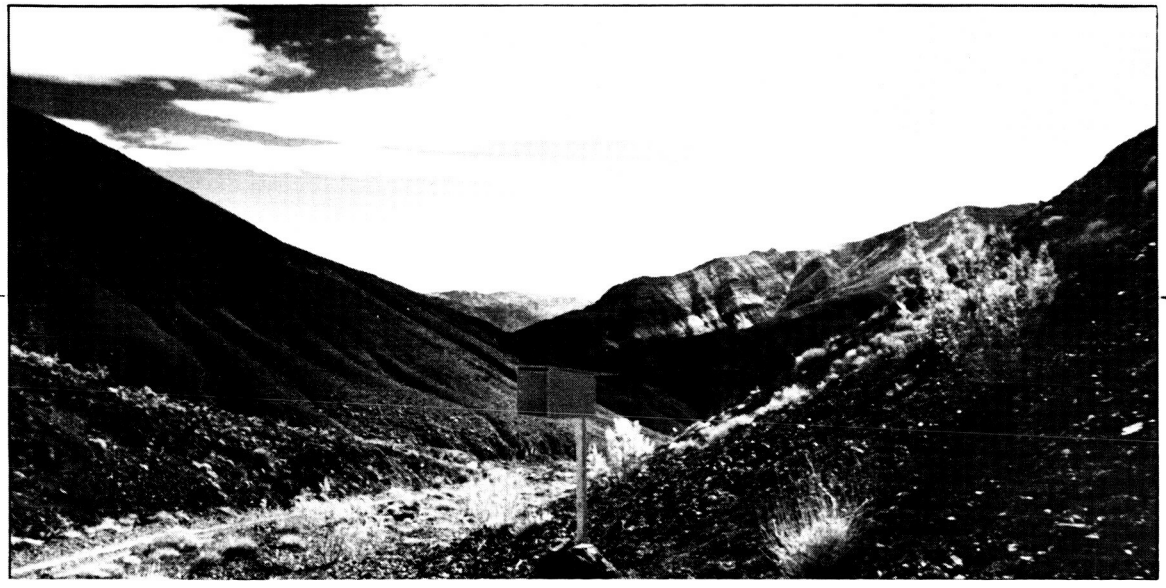

Fig. 14. Thermograph site No. 2 located at an elevation of 5000 ft msl.

Fig. 15. Thermograph site No. 1 located at an elevation of 6000 ft msl.

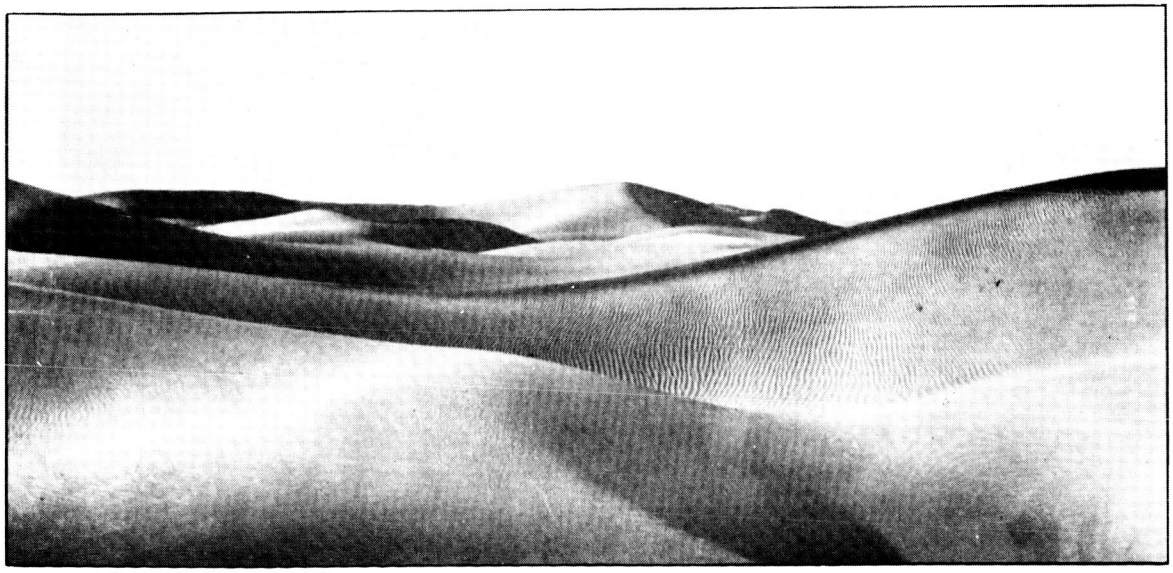

Fig. 16. Death Valley sand dunes situated near Stovepipe Wells.

Fig. 17. Salt Flats located immediately north of the Devils Golf Course.

Fig. 18. Detailed view of the rugged surface terrain at the Devils Golf Course.

Fig. 19. Amargosa Desert located at an average elevation of 2500 ft msl to the east of Death Valley.

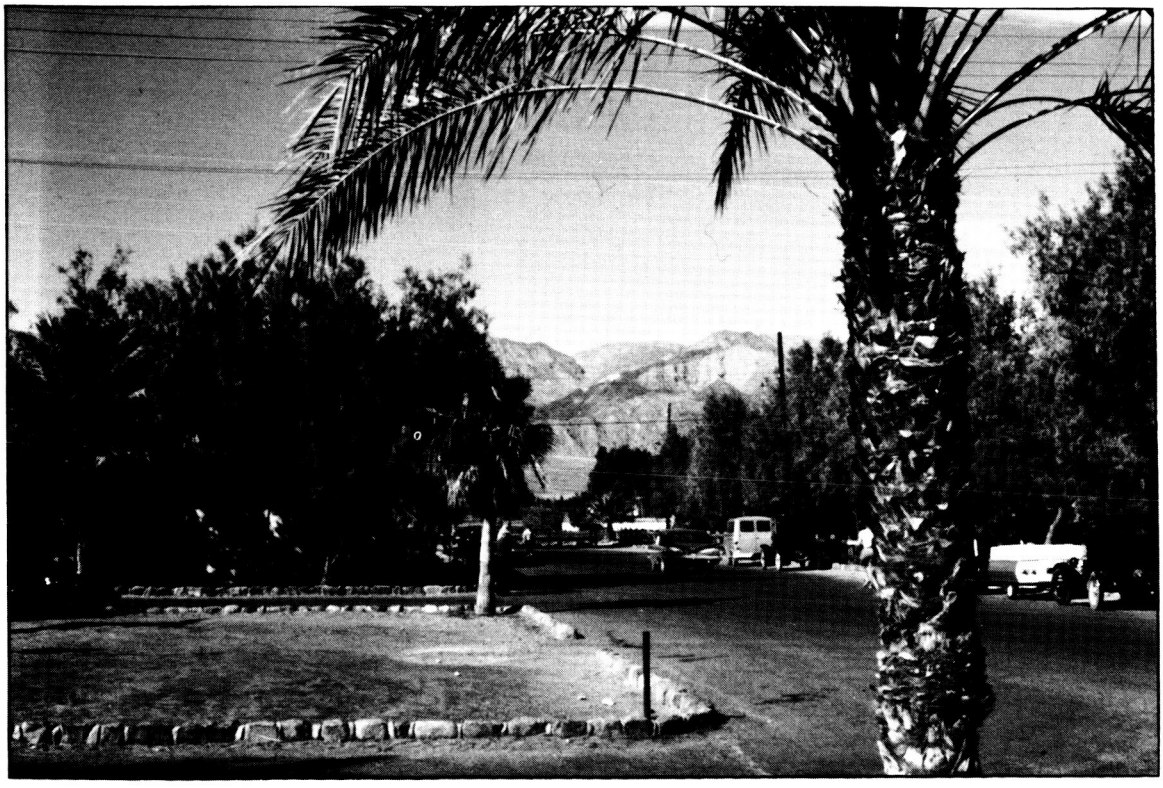

Fig. 20. Furnace Creek Oasis.

MESOMETEOROLOGY PROJECT - - - - - RESEARCH PAPERS

(Continued from front cover)

16. Preliminary Result of Analysis of the Cumulonimbus Cloud of April 21, 1961 -Tetsuya Fujita and James Arnold

17. A Technique for Precise Analysis of Satellite Photographs - Tetsuya Fujita

18. Evaluation of Limb Darkening from TIROS III Radiation Data - S.H.H. Larsen, Tetsuya Fujita, and W. L. Fletcher

19. Synoptic Interpretation of TIROS III Measurements of Infrared Radiation -Finn Pedersen and Tetsuya Fujita

20. TIROS III Measurements of Terrestrial Radiation and Reflected and Scattered Solar Radiation - S.H.H. Larsen, Tetsuya Fujita, and W.L. Fletcher

21. On the Low-level Structure of a Squall Line - Henry A. Brown

22. Thunderstorms and the Low-level Jet - William D. Bonner

23. The Mesoanalysis of an Organized Convective System - Henry A. Brown

24. Preliminary Radar and Photogrammetric Study of the Illinois Tornadoes of April 17 and 22, 1963 - Joseph L. Goldman and Tetsuya Fujita

25. Use of TIROS Pictures for Studies of the Internal Structure of Tropical Storms -Tetsuya Fujita with Rectified Pictures from TIROS I Orbit 125, R/O 128 -Toshimitsu Ushijima

26. An Experiment in the Determination of Geostrophic and Isallobaric Winds from NSSP Pressure Data - William Bonner

27. Proposed Mechanism of Hook Echo Formation - Tetsuya Fujita with a Preliminary Mesosynoptic Analysis of Tornado Cyclone Case of May 26, 1963 -Tetsuya Fujita and Robbi Stuhmer

28. The Decaying Stage of Hurricane Anna of July 1961 as Portrayed by TIROS Cloud Photographs and Infrared Radiation from the Top of the Storm -Tetsuya Fujita and James Arnold

29. A Technique for Precise Analysis of Satellite Data, Volume II - Radiation Analysis, Section 6. Fixed-Position Scanning - Tetsuya Fujita

30. Evaluation of Errors in the Graphical Rectification of Satellite Photographs -Tetsuya Fujita

(Continued on outside)

MESOMETEOROLOGY PROJECT - - - - - RESEARCH PAPERS

(Continued from inside)

31. Tables of Scan Nadir and Horizontal Angles - William D. Bonner

32. A Simplified Grid Technique for Determining Scan Lines Generated by the TIROS Scanning Radiometer - James E. Arnold

33. A Study of Cumulus Clouds over the Flagstaff Research Network with the Use of U-2 Photographs - Dorothy L. Bradbury and Tetsuya Fujita

34. The Scanning Printer and Its Application to Detailed Analysis of Satellite Radiation Data - Tetsuya Fujita

35. Synoptic Study of Cold Air Outbreak over the Mediterranean using Satellite Photographs and Radiation Data - Aasmund Rabbe and Tetsuya Fujita

36. Accurate Calibration of Doppler Winds for their use in the Computation of Mesoscale Wind Fields - Tetsuya Fujita

37. Proposed Operation of Instrumented Aircraft for Research on Moisture Fronts and Wake Depressions - Tetsuya Fujita and Dorothy L. Bradbury

38. Statistical and Kinematical Properties of the Low-Level Jet Stream - William D. Bonner

39. The Illinois Tornadoes of 17 and 22 April 1963 - Joseph L. Goldman

40. Resolution of the Nimbus High Resolution Infrared Radiometer - Tetsuya Fujita and William R. Bandeen

41. On the Determination of the Exchange Coefficients in Convective Clouds - Rodger A. Brown

42. A Study of Factors Contributing to Dissipation of Energy in a Developing Cumulonimbus - Rodger A. Brown and Tetsuya Fujita

43. A Program for Computer Gridding of Satellite Photographs for Mesoscale Research - William D. Bonner

44. Comparison of Grassland Surface Temperatures Measured by TIROS VII and Airborne Radiometers under Clear Sky and Cirriform Cloud Conditions - Ronald M. Reap